

# Shear avalanches in metallic glasses under nanoindentation: Deformation units and rate dependent strain burst cut-off

Cite as: Appl. Phys. Lett. **103**, 101907 (2013); <https://doi.org/10.1063/1.4820782>

Submitted: 23 July 2013 . Accepted: 21 August 2013 . Published Online: 06 September 2013

X. L. Bian, G. Wang, K. C. Chan, J. L. Ren, Y. L. Gao, and Q. J. Zhai



View Online



Export Citation



CrossMark

## ARTICLES YOU MAY BE INTERESTED IN

[Serrated flow behaviors of a Zr-based bulk metallic glass by nanoindentation](#)

Journal of Applied Physics **115**, 084907 (2014); <https://doi.org/10.1063/1.4866874>

[Dynamics of serrated flow in a bulk metallic glass](#)

AIP Advances **1**, 032158 (2011); <https://doi.org/10.1063/1.3643218>

[Correlations between elastic moduli and properties in bulk metallic glasses](#)

Journal of Applied Physics **99**, 093506 (2006); <https://doi.org/10.1063/1.2193060>

Lock-in Amplifiers  
Find out more today



Zurich  
Instruments

AIP  
Publishing

# Shear avalanches in metallic glasses under nanoindentation: Deformation units and rate dependent strain burst cut-off

X. L. Bian,<sup>1</sup> G. Wang,<sup>1,a)</sup> K. C. Chan,<sup>2</sup> J. L. Ren,<sup>3</sup> Y. L. Gao,<sup>1</sup> and Q. J. Zhai<sup>1</sup>

<sup>1</sup>Laboratory for Microstructures, Shanghai University, Shanghai 200444, China

<sup>2</sup>Department of Industrial and System Engineering, the Hongkong Polytechnic University, Kowloon, Hongkong

<sup>3</sup>School of Mathematics and Statistics, Zhengzhou University, Zhengzhou 450001, China

(Received 23 July 2013; accepted 21 August 2013; published online 6 September 2013)

Indented metallic glasses at the nanoscale deform via strain bursts. Conventional continuum descriptions are not appropriate for such highly stochastic, intermittent deformations. In this study, after a statistical analysis of strain bursts in five metallic glasses, the dependence of the cut-off of the strain burst size on deformation units and loading rate is established. For soft metallic glasses with smaller deformation units, cut-off of the strain burst size truncates the scale-free behavior at larger strain burst sizes. For hard metallic glasses, scale-free behavior occurs in a wide range of strain burst sizes. © 2013 AIP Publishing LLC. [<http://dx.doi.org/10.1063/1.4820782>]

The plastic deformation in crystalline materials exhibits intermittent strain bursts, i.e., slip avalanches, with a scale-free size distribution at the microscale.<sup>1–3</sup> Some large slip avalanches are also usually visible in macroscale deformation,<sup>3,4</sup> which can seriously influence the mechanical properties of crystalline materials. These slip avalanches are associated with intrinsic hardening of the material,<sup>3</sup> grain size<sup>4</sup> or test sample geometric size, and so on.<sup>5</sup> In metallic glasses, grain size and the hardening behavior do not exist. Close resemblance to the crystalline plasticity characterized by disruptive shock-and-aftershock, and earthquake-like events over spatio-temporal averages at the nanoscale, the shear banding behavior in metallic glasses corresponds to intermittent shear avalanches with different sizes.<sup>6–8</sup> Such a shear avalanche is a fatal event resulting in a catastrophic fracture and tiny plastic strain (<2%) for metallic glasses.<sup>9</sup> Prohibiting shear avalanches could enhance the toughness of metallic glasses and promote their plasticity.<sup>8</sup> Shear banding in metallic glasses is associated with environmental temperatures,<sup>10</sup> elastic properties,<sup>11</sup> and inhomogeneities in the glassy phase.<sup>12,13</sup> As spatio-temporal nonlinear dynamic behavior, shear banding must be spatially influenced by the deformation units in the glassy phase, and also temporally affected by the external driving rate,<sup>10</sup> which dependencies remain unclear so far. Therefore, understanding and predicting the dependence of shear avalanches on the atomic structure and loading rate are the questions to be addressed here.

In this letter, we use nanoindentation to investigate the strain bursts in the loading stage of metallic glasses. High spatial and temporal resolution in the instrumented nanoindentation allows us to explore the discontinuous strain burst in different metallic glasses.<sup>14</sup> A statistical analysis is conducted for the strain burst size distribution. The influences of the deformation unit and the loading rate of the metallic glasses on the strain burst are discussed.

Five metallic glasses are chosen according to their different mechanical properties, such as hardness and elastic modulus, namely  $\text{Co}_{56}\text{Ta}_9\text{B}_{35}$  (at. %),

$\text{Fe}_{41}\text{Co}_7\text{Cr}_{15}\text{Mo}_{14}\text{C}_{15}\text{B}_6\text{Y}_2$ ,  $\text{Zr}_{41.25}\text{Ti}_{13.75}\text{Ni}_{10}\text{Cu}_{12.5}\text{Be}_{22.5}$ ,  $\text{Mg}_{65}\text{Cu}_{25}\text{Gd}_{10}$ , and  $\text{Ce}_{68}\text{Al}_{10}\text{Cu}_{20}\text{Co}_2$  metallic glasses. The experimental procedures are described in Ref. 15. According to the results from the nanoindentation tests, the elastic modulus,  $E$ , and the hardness,  $H$ , of the five metallic glasses are measured from the average of ten  $P$ - $h$  curves at each loading rate, as listed in Table I. Based on the hardness values, we call the Co- and Fe-based types as “hard” metallic glasses, and the Zr-, Mg-, and Ce-based types as “soft” metallic glasses. The representative load-displacement ( $P$ - $h$ ) curves at five loading rates for “hard” (Co-based) and “soft” (Mg-based) metallic glasses are plotted in Figs. 1(a) and 1(b). The  $P$ - $h$  curves of the other three metallic glasses are plotted in Fig. S1.<sup>15</sup> The  $P$ - $h$  curves of the hard metallic glasses are seen to be smooth in the loading stage without obvious shear steps. On further enlarging of the loading stages, some very small pop-in events can be observed [the inset of Fig. 1(a)]. For the soft metallic glasses, significant pop-in events in the loading stage [as marked by black arrows in Fig. 1(b)] are visible.

To further characterize these pop-in events, it requires eliminating the influences from the indentation depth increase. A polynomial function is used to fit the loading stage in  $P$ - $h$  curves to get a baseline [Fig. 1(c)]. After subtraction of the baseline, the pop-in events as a function of the  $h$  value are visible. Since each pop-in event reflects a process of shear band formation and propagation,<sup>14</sup> the depth drop,  $\Delta h$ , i.e., difference between the peak and valley values [as marked in the inset of Fig. 1(c)], can reflect the shear step size. However, the instrument noise could also cause pop-in events, and is required to be removed. The pop-in events from the background noise can be extracted from the 5 s holding segment at peak load through linear fitting that is well documented in Fig. S2(a),<sup>15</sup> which shows that the noise generates a shear step size of 2 nm [as marked in Fig. S2(b)].<sup>15</sup> Thus, the pop-in events with shear step sizes less than 2 nm are not considered in the present study. After removing the noise, normalization of the  $\Delta h$  value by the depth,  $h$ , is carried out to eliminate the statistical error, which generates strain burst size,  $S$ , ( $=\Delta h/h$ ).<sup>14</sup> The distributions of

<sup>a)</sup> Author to whom correspondence should be addressed. Electronic mail: g.wang@shu.edu.cn

TABLE I. Parameters for the five metallic glasses.  $\rho_m$  is mass density;  $E$  is elastic modulus;  $G$  is shear modulus;  $H$  is hardness.

Metallic glasses	$\rho_m$ (g/cm <sup>3</sup> )	$E$ (GPa)	$G$ (GPa)	$H$ (GPa)
Co-based	9.285	293	111.53	16.4
Fe-based	7.904	256	97.78	13.8
Zr-based	6.125	90	32.81	5.6
Mg-based	3.794	60	22.85	2.9
Ce-based	6.752	45	16.94	2.8

the  $S$  value versus the  $h$  value from five metallic glasses at a loading rate of 0.6 mN/s are representatively plotted in Fig. 1(d). It is evident that the sizes of the strain bursts of the five metallic glasses exhibit random fluctuations although the size distributions seem to be a decreasing trend with increasing indentation depth.

Considering the distribution of the strain burst is irregularly and stochastically changing across the variant metallic glasses, we carry out a statistic analysis on the strain burst size, attempting to gain a better understanding of the mechanism despite the characteristic lack of periodicity in the intermittent pop-in events. Ergodically processing is introduced to demonstrate the statistic distributions of the strain burst size. Figure 2 shows cumulative probability distributions of the strain burst sizes, i.e., the percentage of the number of pop-in events with the strain burst size being larger than a given value,  $P(>S)$ , for the five metallic glasses loaded at different rates. It can be seen that the smaller strain bursts are more probable and follow a power-law distribution. For a metallic glass indented at a given loading rate, with increasing the strain burst size, the distributions of the strain burst sizes do not follow a power-law distribution but decrease exponentially in probability. Using a Levenberg-Marquardt algorithm, the cumulative probability distributions of the five metallic glasses can be predicted by an empirical relation<sup>4</sup>

$$P(>S) = AS^{-\beta} \exp(-S/S_C), \quad (1)$$

where  $A$  is a normalization constant,  $S$  is the strain burst,  $\beta$  is a scaling exponent, and  $S_C$  is the cut-off of strain burst size. The fitting parameters,  $\beta$  and  $S_C$ , reflect the profile of the shear avalanche in metallic glasses.<sup>4</sup>

For metallic glasses, with good ductility, subjected to a compression load, the dynamics of the collective shear banding can self-organize into a scale-free pattern characterized by a power-law distribution of shear avalanche sizes,  $P(>S) \sim S^{-\beta}$ , with the exponent of  $\beta$  being around 1.5.<sup>14,16</sup> This confirms the high degree of universality of the observed power-law relation, reminiscent of self-organized critical (SOC) behavior. Under nanoindentation, due to the confinement from the surrounding material, plastically shearing can be stabilized even in brittle metallic glasses without any compression plasticity,<sup>17</sup> which sheds light on the characteristics of the intermittent shear avalanches. The  $\beta$  values are varied for different metallic glasses but are kept constant at different loading rates for each metallic glass, and are shown in Fig. 2. For the hard metallic glasses, their  $\beta$  values are 0.65 and 1.00, respectively. They exhibit a significant power-law relation in the small size regime of the strain bursts [Figs. 2(a) and 2(b)]. With increasing strain burst size up to a larger value, i.e., the cut-off value of  $S_C$ , the exponential decay factor comes to play. For the soft metallic glasses, the power-law regime is not really significant as the cut-off has noticeably decreased to smaller values. Thus, smaller exponents of 0.20 and 0.10 could be seen [Figs. 2(c)–2(e)]. It is evident that the changes in the  $\beta$  value are influenced by the cut-off of the strain burst size. As a characteristic strain burst size,  $S_C$ , in Eq. (1) can reflect the shear avalanche occurring in the large scale,<sup>18</sup> which is of important in the rupture process of crystalline materials.<sup>3,4,18</sup>

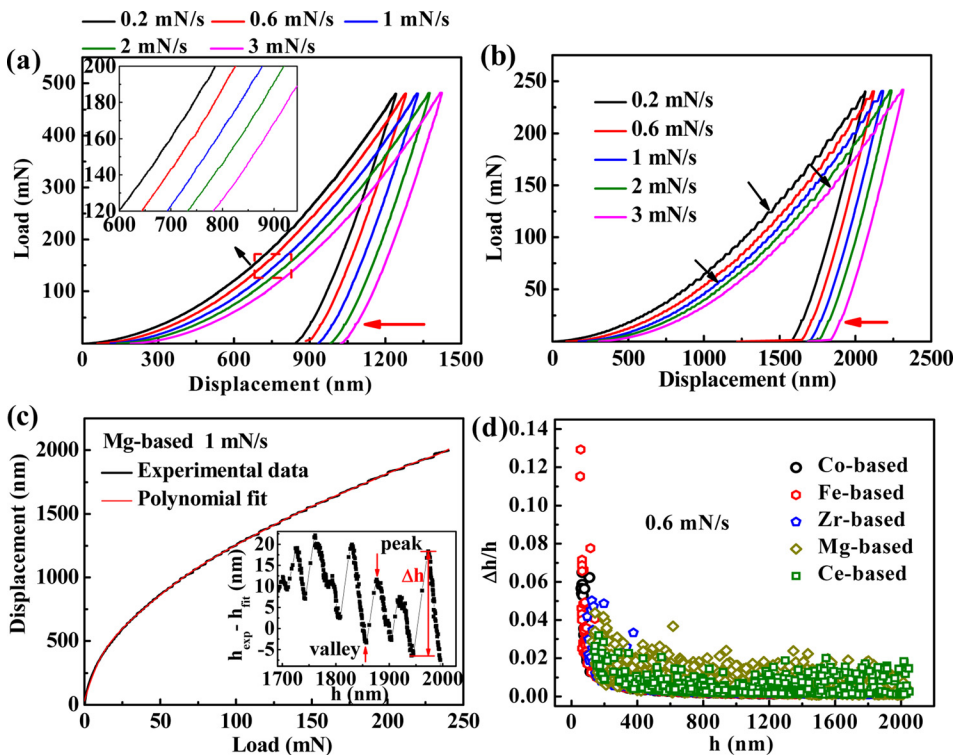


FIG. 1. Load-displacement ( $P$ - $h$ ) curves during nanoindentation at various loading rates for different metallic glasses. (a) The  $P$ - $h$  curves of the Co-based metallic glass at five loading rates. (b) The  $P$ - $h$  curves of the Mg-based metallic glass at five loading rates. The start points of the curves are offset for clearer viewing in (a) and (b). (c) Polynomial function fitting curve of the displacement-load for the loading segment on Mg-based metallic glass at the loading rate of 1 mN/s. The inset shows the serration events. (d) Strain burst size distribution as a function of depth of the five metallic glasses at the loading rate of 0.6 mN/s.

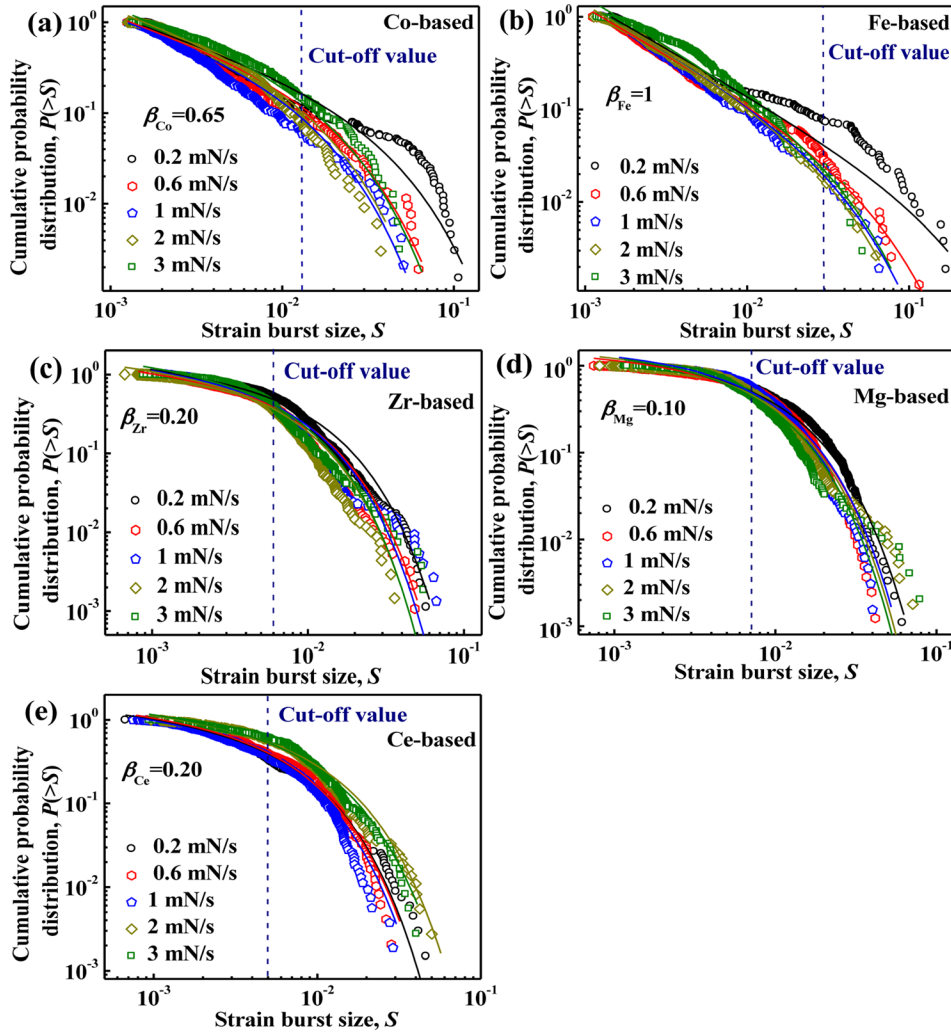


FIG. 2. Cumulative probability distributions of strain burst size. Open scattering points represent experimental results measured from the nanoindentation. Solid lines are fitting curves by Eq. (1). (a) Co-based, (b) Fe-based, (c) Zr-based, (d) Mg-based, and (e) Ce-based.

Since no crystallographic defects can deliver plastic strain, the structural origin of the deformation in metallic glasses is attributed to deformation units, such as shear transformation zones.<sup>19,20</sup> The deformation unit operation includes a group of atoms concordantly shifting and forming a concordant region.<sup>21</sup> The stress increase can bring out an expansion of this concordant region due to more atoms participating in rearrangement.<sup>21</sup> In the nanoindentation, the load increase in each pop-in event corresponds to the concordant region expansion. After the load approaches the peak value, the expansion of the concordant region is in a jamming state because of the elastic field interactions between neighboring concordant regions.<sup>22,23</sup> On the other hand, the enlarged concordant region brings out larger internal stress concentration.<sup>24</sup> When this stress concentration is larger than the yield shear stress, shear banding can slide a given distance, thus, intermittent pop-in behavior is formed. The formation of the concordant region is actually a response of the metallic glass to the external elastic load, which is manifested in a redistribution of the local stresses in an elastic medium.<sup>25,26</sup> This stress redistribution is carried out by an elastic interaction between atoms over a distance of shear wave propagation.<sup>27</sup> Thus, the concordant region size,  $d$ , can be assumed to be  $d = v_s \tau$ , where  $v_s$  is the shear wave speed, and  $\tau$  is the relaxation time that depends on the temperature. In the present study, the  $\tau$  value (approximately 1 ~ 2 ps) is

a constant since the experiments were carried out at room temperature.<sup>27</sup> The shear wave speed can be calculated by  $v_s = (G/\rho)^{1/2}$ , where  $G$  and  $\rho$  are the shear modulus and density of the metallic glasses, respectively, which are listed in Table I. Accordingly, it can be seen that the concordant region size is determined by the propagation of the shear wave,<sup>26</sup> which further indicates that the shear banding behavior is related to the shear wave propagation. Figure 3 plots the relationship between the shear wave speed and the

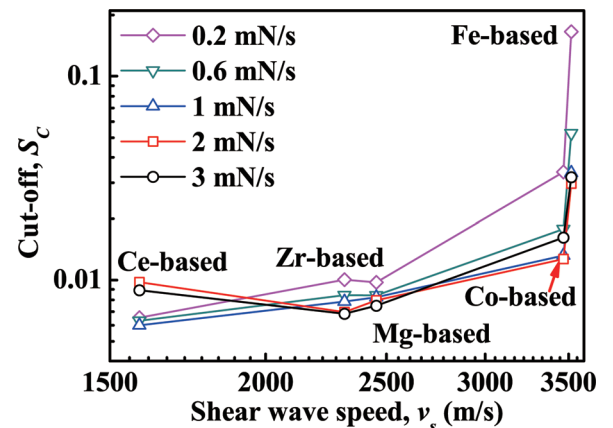


FIG. 3. Cut-off values of strain burst size as a function of shear wave speed at different loading rates and different metallic glasses.



cut-off of the strain burst size of five metallic glasses at different loading rates. The cut-off value increases with increasing shear wave speed. For a metallic glass, the higher the loading rate, the smaller the cut-off value, which is analogous to the result of a previous study.<sup>4</sup>

Larger shear wave speed suggests that more atoms will participate in the concordant shifting, which causes a higher activation energy corresponding to higher hardness (strength) in metallic glasses, such as the Co- and Fe-based metallic glasses. In the loading stage of each pop-in event, the samples with larger concordant regions can more easily form a jamming configuration compared to those with a smaller concordant region because the larger long-range elastic strain fields initiated from different concordant regions encounter each other more easily.<sup>28</sup> For the soft metallic glasses, their concordant regions are smaller in size, which means that the jammed state of the deformation units is weakened. Therefore, by increasing the hardness, the deformation units exhibit an unjamming-jamming transition in metallic glasses. This transition can be viewed as an extension of the idea of the rigidly packed deformation units (concordant regions) in a jammed state.<sup>29,30</sup> This rigid packing state can resist small perturbations,<sup>31</sup> approaching a stable state, i.e., a non-chaotic state. The cumulative probability distributions of the strain burst size in hard metallic glasses clearly show the significant power-law relation in a wide range of strain burst sizes, suggesting a SOC state, i.e., one of stable states, occurring [Figs. 2(a) and 2(b)]. This provides solid evidence to support the idea that the large concordant region formed a jamming state. With decreasing the deformation unit size, the transition from jamming to unjamming states occurs. The un-jamming state is unstable to perturbations, exhibiting a chaotic state,<sup>18</sup> which is manifested in the power-law relation in the statistic distribution of strain bursts that is not obvious due to the influence from smaller cut-off values. This confirms the conjecture of the transition of the jamming-unjamming processes.

Increasing the loading rate causes the cut-off values to decrease (Fig. 3). At the lower loading rate, a shear band formation is assumed to render the plastic strain, leading to a strain burst.<sup>32</sup> Increasing the loading rate to be larger than the rate of relaxation by a single shear band, besides a new shear band operation, the previous shear band will also be operatable as the stress level exceeds the yield criterion again, so two shear bands are initiated. Further increasing the loading rate, numerous shear bands would be formed at each pop-in event to dissipate the plastic strain. We can then image a virtual shear band cloud continuously rendering the imposed strain and cutting the elastic energy accommodation in each pop-in event. Thus, the amplitude of a pop-in event is smaller with increasing load rate, causing the cut-off values to decrease. The changes of the cut-off values do not significantly influence the  $\beta$  value in each metallic glass. A possible reason is that the range of loading rates in the present study is too small to change the dynamic behavior of the shear banding process.<sup>33</sup>

In summary, unlike crystalline materials having crystalline defects to confine the shear avalanche at the microscale, metallic glasses whilst having no defects, the plastic flow under nanoindentation shows that the cut-off of the strain burst size, corresponding to the shear avalanche size, is

associated with the deformation unit size in the glassy phase. This deformation unit size is determined by the shear wave propagation distance. The loading rates cannot influence the cumulative probability distribution of the strain burst size.

The stimulated discussions with Professor W. H. Wang at the Institute of Physics, CAS, are acknowledged. The work described in this paper was supported by grants from NSF of China (Nos. 51171098, 51222102, and 11271339), the RGC of the Hong Kong (No. PolyU511211), the Shanghai Pujiang Program (No. 11PJ1403900), the Innovation Program of Shanghai Municipal Education Commission (No. 12ZZ090), the Program for Professor of Special Appointment (Eastern Scholar) at Shanghai Institutions of Higher Learning, and the 085 project in Shanghai University.

<sup>1</sup>D. M. Dimiduk, C. Woodward, R. LeSar, and M. D. Uchic, *Science* **312**, 1188 (2006).

<sup>2</sup>M. C. Miguel, A. Vespignani, S. Zapperi, J. Weiss, and J.-R. Grasso, *Nature* **410**, 667 (2001).

<sup>3</sup>M. Zaiser and P. Moretti, *J. Stat. Mech.: Theory Exp.* **2005**, P08004.

<sup>4</sup>T. Richeton, J. Weiss, and F. Louchet, *Nature Mater.* **4**, 465 (2005).

<sup>5</sup>M. Zaiser and N. Nikitas, *J. Stat. Mech.: Theory Exp.* **2007**, P04013.

<sup>6</sup>K. A. Dahmen, Y. Ben-Zion, and J. T. Uhl, *Nature Phys.* **7**, 554 (2011).

<sup>7</sup>B. A. Sun, S. Pauly, J. Tan, M. Stoica, W. H. Wang, U. Kühn, and J. Eckert, *Acta Mater.* **60**, 4160 (2012).

<sup>8</sup>G. Wang, K. C. Chan, L. Xia, P. Yu, J. Shen, and W. H. Wang, *Acta Mater.* **57**, 6146 (2009).

<sup>9</sup>M. F. Ashby and A. L. Greer, *Scr. Mater.* **54**, 321 (2006).

<sup>10</sup>D. Klaumünzer, A. Lazarev, R. Maaß, F. H. D. Torre, A. Vinogradov, and J. F. Löffler, *Phys. Rev. Lett.* **107**, 185502 (2011).

<sup>11</sup>J. C. Ye, J. Lu, C. T. Liu, Q. Wang, and Y. Yang, *Nature Mater.* **9**, 619 (2010).

<sup>12</sup>W. H. Wang, *Prog. Mater. Sci.* **57**, 487 (2012).

<sup>13</sup>J. Das, M. B. Tang, K. B. Kim, R. Theissmann, F. Baier, W. H. Wang, and J. Eckert, *Phys. Rev. Lett.* **94**, 205501 (2005).

<sup>14</sup>B. A. Sun, H. B. Yu, W. Jiao, H. Y. Bai, D. Q. Zhao, and W. H. Wang, *Phys. Rev. Lett.* **105**, 035501 (2010).

<sup>15</sup>See supplementary materials at <http://dx.doi.org/10.1063/1.4820782> for details about the experimental procedures, the load-displacement ( $P$ - $h$ ) curves, the determination of the instrument noises, and the strain burst size distributions as a function of indentation depth.

<sup>16</sup>J. L. Ren, C. Chen, Z. Y. Liu, R. Li, and G. Wang, *Phys. Rev. B* **86**, 134303 (2012).

<sup>17</sup>C. A. Schuh, J. K. Mason, and A. C. Lund, *Nature Mater.* **4**, 617 (2005).

<sup>18</sup>S. Papanikolaou, D. M. Dimiduk, W. Choi, J. P. Sethna, M. D. Uchic, C. F. Woodward, and S. Zapperi, *Nature* **490**, 517 (2012).

<sup>19</sup>W. L. Johnson and K. Samwer, *Phys. Rev. Lett.* **95**, 195501 (2005).

<sup>20</sup>Z. Wang, P. Wen, L. S. Huo, H. Y. Bai, and W. H. Wang, *Appl. Phys. Lett.* **101**, 121906 (2012).

<sup>21</sup>G. Wang, N. Mattern, J. Bednarčík, R. Li, B. Zhang, and J. Eckert, *Acta Mater.* **60**, 3074 (2012).

<sup>22</sup>N. D. Denkov, S. Tcholakova, K. Golemanov, and A. Lips, *Phys. Rev. Lett.* **103**, 118302 (2009).

<sup>23</sup>P. Hähner and M. Zaiser, *Acta Mater.* **45**, 1067 (1997).

<sup>24</sup>D. Pan, A. Inoue, T. Sakurai, and M. W. Chen, *Proc. Natl. Acad. Sci. U.S.A.* **105**, 14769 (2008).

<sup>25</sup>W. Dmowski, T. Iwashita, C.-P. Chuang, J. Almer, and T. Egami, *Phys. Rev. Lett.* **105**, 205502 (2010).

<sup>26</sup>V. A. Levashov, J. R. Morris, and T. Egami, *Phys. Rev. Lett.* **106**, 115703 (2011).

<sup>27</sup>K. Trachenko, *Phys. Rev. B* **75**, 212201 (2007).

<sup>28</sup>M. F. Ashby, *Philos. Mag.* **21**, 399 (1970).

<sup>29</sup>C. S. O'Hern, L. E. Silbert, A. J. Liu, and S. R. Nagel, *Phys. Rev. E* **68**, 011306 (2003).

<sup>30</sup>M. Wyart, S. R. Nagel, and T. A. Witten, *Europhys. Lett.* **72**, 486 (2005).

<sup>31</sup>E. J. Banigan, M. K. Illich, D. J. Stace-Naughton, and D. A. Egolf, *Nature Phys.* **9**, 288 (2013).

<sup>32</sup>C. A. Schuh and T. G. Nieh, *Acta Mater.* **51**, 87 (2003).

<sup>33</sup>H. Li, A. H. W. Ngan, and M. G. Wang, *J. Mater. Res.* **20**, 3072 (2005).